Controllable Nd2Fe14B/α-Fe Nanocomposites: Chemical Synthesis and Magnetic Properties

Journal:	*Nanoscale*
Manuscript ID:	NR-ART-04-2014-002163.R1
Article Type:	Paper
Date Submitted by the Author:	25-Jun-2014
Complete List of Authors:	Yu, Lianqing; China University of Petroleum, Yang, Ce; Peking University, Department of Materials Science and Engineering, Hou, Yanglong; Peking University, Department of Materials Science and Engineering,

WILEY-VCH

DOI: 10.1002/ ((please add manuscript number))
Article type: Full Paper

Controllable $Nd_2Fe_{14}B/\alpha\text{-}Fe$ Nanocomposites: Chemical Synthesis and Magnetic Properties

*Lianqing Yu, Ce Yang, and Yanglong Hou**

[*] Prof. Y. Hou, C. Yang
Department of Materials Science and Engineering, College of Engineering, Peking University
Beijing 100871, China
E-mail: hou@pku.edu.cn
Dr. L.Q. Yu
Department of Materials Science and Engineering, College of Engineering, Peking University
Beijing 100871, China
College of Science, China University of Petroleum
Qingdao 266580, China

Keywords: Exchange-coupled, nanocomposites, NdFeB, reductive annealing process, chemical synthesis

It is extremely desirable but challenging to develop exchange-coupled magnets with well dispersed hard/soft phase and confined size to meet the high energy requirements of advanced magnets in modern industry and information technology. Here, we report a novel bottom up strategy with two-step thermal decomposition and reductive annealing process to synthesize $Nd_2Fe_{14}B/\alpha\text{-}Fe$ nanocomposites, in which effective control of the hard/soft magnetic phase size and proportion were achieved. It is worth noting that the composition as well as phase distribution can be readily tuned by changing the ratio between Nd-Fe-B-oxide and α-Fe. This work provides an effective approach to adjusting phase size and distribution for exchange-coupled rare earth nanomagnets, which can be fundamental for high energy magnets.

1. Introduction

Rare earth (RE)–transition metal intermetallics with highly ferromagnetic performance have attracted intensive interests because they have been widely used in aerospace, motors, electronics and automotive industries. However, because of the scare resources and large cost of RE elements, there is strong demand to develop permanent magnets containing smaller amounts of RE elements to achieve superior maximum energy products. Interestingly, exchange-coupling phonemenon provides a new access to the objective magnets.[1a, 1b] In the exchange-coupled magnets, a large maximum energy product, $(BH)_{max}$, is expected when the two phases are fully exchange-coupled by refining the grain sizes of the soft magnetic phase to about twice the domain wall width of the hard phase (≈10 nm).[2]

$Nd_2Fe_{14}B$-based nanocomposites containing exchange-coupled magnetic hard and soft phases are considered to be desirable permanent magnets for their large coercivity, high magnetization, and enhanced maximum energy product.[3a, 3b] Very recently, Hono et al. obtained a $(BH)_{max}$ of 486 kJ m^{-3} in $Nd_2Fe_{14}B$/FeCo nanocomposite films by carefully tuning the ratio of hard and soft phases *via* physical sputtering method.[4] Although the interphase between hard and soft magnetic phases, which is the core for the effective exchange-coupling, can be easily manipulated in preparation of thin film magnets[4, 5], this is tough to be realized in preparation of high performance bulk magnetic nanocompsites[6a, 6b], which are deadly required in various industry applications.

In past decade, there is significant progress in synthesis of magnetic nanoparticles (NPs) with controlled size and morphology by using high temperature wet chemical approach.[7a, 7b, 7c] And this provides scientists a promising approach to manage the exchange-coupling effect through a precisely established bottom-up strategy. Zeng et al. have demonstrated self-assembly of hard magnetic FePt and soft magnetic Fe_3O_4 NPs with strong exchange-coupling effect to enhance $(BH)_{max.}$[2] Hong et al. prepared a core/shell type structure of effective exchange-coupled $Sm(Co_{1-x}Fe_x)_5/Fe_3O_4$ (x=0.1).[8] By combining wet chemical synthesis and Ca-assisted high temperature reduction processes, we obtained $SmCo_5/Fe_x$ (x=0-2.9) nanocomposites with tuned magnetic properties by controlling the composition and grain size of Fe_3O_4 nanoparticles.[9a, 9b] Deheri and co-workers synthesized $Nd_2Fe_{14}B$ NPs of ~65 nm by sol-gel based method,[10] but, the particle is beyond the critical radium for exchange-coupling effect. In fact, many efforts have been tried to obtain nano-sized $Nd_2Fe_{14}B$ *via* wet chemical method. However, due to the high negative reduction potential of Nd^{3+}/Nd (-2.323 eV vs SHE) and easily oxidation of $Nd_2Fe_{14}B$ powder, the synthesis of $Nd_2Fe_{14}B$ NPs and nanocomposite powder is extremely challenging.

Here, we report a facile chemical approach to fabricate well exchange-coupled $Nd_2Fe_{14}B$/α-Fe nanocomposites by effective control of the hard/soft magnetic phase size and proportio, which might provide an effective route to manipulate exchange-coupling interactions in the nanocomposites. Scheme 1 shows a schematic illustration of synthetic process of NdFeB/α-Fe nanocomposites. In our strategy, monodisperse α-Fe NPs were firstly synthesized by thermal decomposition of $Fe(CO)_5$.[11] Afterwards, the obtained Fe NPs were added into oleylamine(OAm)-contained organic precursors of Nd, Fe, B. The mixture was subsequently heated to 300 ℃ to generate Nd-Fe-B-oxide/α-Fe composite. Finally, with a subsequent Ca-assisted high temperature reductive annealing process, the as-synthesized Nd-Fe-B-oxide/α-Fe composites were further converted into $Nd_2Fe_{14}B$/α-Fe exchange-coupled magnets in which the composition as well as magnetic properties are able to be tuned by changing the ratio between Nd-Fe-B-oxide and α-Fe.

2. Results and Discussion

Monodisperse α-Fe NPs were prepared by thermal decomposition of $Fe(CO)_5$,[12] a type of transmission electron microscopy (TEM) image of samples is shown in Figure 1a, the average size of sample is 5 nm (Figure S1), and XRD pattern (Figure 1b) confirmed the chemical structure of sample as α-Fe. The Nd-Fe-B-oxide/α-Fe nanocomposites were synthesized by the co-decomposition of $Nd(acac)_3$, $Fe(acac)_3$ and $(C_2H_5)_3NBH_3$ with the existence of α-Fe NPs. TEM was also applied to investigate structures of the Nd-Fe-B-oxide/α-Fe nanocomposites. As shown in Figure 1c and d, it can be seen that α-Fe NPs are well-dispersed and uniformly embedded in net-like Nd-Fe-B-oxide matrix. To prepare the exchange-coupled magnets, the Nd-Fe-B-oxide/α-Fe composites were subsequently annealed under 850℃ for 1.5 h under Ar/H_2 atmosphere with Ca as reducing agent. X-ray diffraction (XRD) patterns of the resulted product were shown in Figure 2. The product can be indexed as tetragonal structural $Nd_2Fe_{14}B$ phase (JCPDS No.36-1296) and α-Fe phase (JCPDS No. 06-0696), suggesting that the $Nd_2Fe_{14}B$/α-Fe magnets were generated after reductive annealing process. The correlated crystalline size of $Nd_2Fe_{14}B$ and α-Fe was estimated to be 25 nm and 10nm from the (410) and (110) diffraction peak using Scherrer's formula, respectively. To identify the composition of the nanocomposite magnets, inductively coupled plasma spectroscopy (ICP) and energy dispersive X-ray spectroscopy (EDS) were utilized. The ICP test showed that the average Fe/Nd ratio of the nanocomposite is 1.38: 10, while the EDS study of a random portion of the product exhibited a homologous result of 1.42: 10 (Figure S2), which is in agreement with ICP data. High resolution transmission electron microscopy (HRTEM) images also manifested the formation of $Nd_2Fe_{14}B$/α-Fe nanocomposite. A typical HRTEM image of $Nd_2Fe_{14}B$/α-Fe composites was shown in Figure 3. It can be seen that the nanoscale domains have various structural orientations. The lattice spacing value of 0.203nm can be indexed to the (110) planes of α-Fe (interplane distance at 0.2027nm, JCPDS No. 06-0696), and the lattice spacing values of 0.219nm, 0.245nm and 0.256nm can be assigned to the (410), (214) and (204) planes of $Nd_2Fe_{14}B$ (interplane distance at 0.213nm, 0.241nm and 0.252nm, respectively, JCPDS No. 36-1296). Moreover, the HRTEM image also implies the α-Fe nanocrystals are well-distributed in $Nd_2Fe_{14}B$ matrix even after high temperature reductive annealing process, which could be attributed to the fact that the Nd-Fe-B-oxide matrix could inhibit the crystal growth as well as α-Fe NPs aggregation. Thus, in the nanocomposite powder, there strained size of well dispersed α-Fe (~8 nm) ensured the effective exchange-coupling between α-Fe and hard magnetic phase.[13a, 13b, 13c, 13d] As increased the α-Fe NPs size to 10nm prepared by $Fe(CO)_5$, the final size of soft phase α-Fe of the nanocomposite enhanced to ~15 nm (Figure S3). Moreover, the composition of as-synthesized nanocomposite magnets can be further tuned by changing the amount of incorporated Nd(acac)$_3$ and annealing conditions. As less Nd source was incorporated (with ratio of Nd/Fe at 1.3/10, Figure S4), the products can be indexed to $Nd_2Fe_{14}B$ and α-Fe phase, but the peak at 44.6^0 indicated that the α-Fe had higher proportion in the nanocomposites (Figure S5). While the segregation of α-Fe could easily happen as reduction & diffusion process at higher temperature or longer time, which led to even much stronger peak of α-Fe (Figure S6) and thus, more diffusion or large grain of α-Fe deteriorated exchange-coupling effect.

The magnetic properties of $Nd_2Fe_{14}B$/α-Fe magnets were characterized by hysteresis loop, as shown in Figure 4. The product (Figure 4a, square curve) showed ferromagnetic feature with a single-phase behavior, indicating the effective exchange-coupling in the nanocomposite powder. In addition, the nanocomposite exhibited a large coercivity H_c of 12000Gs, an enhanced remanence M_r of 45 emu/g with M_r/M_{3T}=0.63. However, when less Nd(acac)$_3$ source was incorporated in the composite precursor, the powder cannot couple effectively, which may ascribe to the aggregation of α-Fe nanocrystals led by the deficiency of $Nd_2Fe_{14}B$ matrix. As a result, the hysteresis loop shows a two-phase separated behavior (Figure 4a, circle curve). The magnetic properties of $Nd_xFe_{10}B_1$ composite with tuned other Nd/Fe ratio were shown in Figure 5. An addition of Nd increases the coercivity to the maximum value of 12000Gs at x=2.6. This may be caused by the fact that Fe nanoparticles are well isolated by net-like Nd-Fe-B-oxide matrix, and thus leading to strong exchange-coupling. While the monotonous decrease remanence can be attributed to the proportional decrease of ferromagnetic element.

The δM-H measurements are commonly used to verify the exchange-coupling effect.[14] δM is defined as $M_d(1-2M_i)$, where M_d is the reduced d_c demagnetization remanence curve and M_i is the reduced isothermal remanence curve. For single-phase nanomagnets, δM always possesses high positive values, suggesting an exchange-coupling interactions, which will suddenly decrease to zero or negative value during the reverse of magnetic field as a result of the cooperative switching of the exchange-coupled grains.[15a, 15b] Figure 4c was a plot of δM versus magnetic field of the as-synthesized $Nd_2Fe_{14}B/\alpha\text{-}Fe$ nanocomposite magnet. As shown in Figure 4, initially δM was positive due to the existence of exchange-coupling effect, and then it became negative after the reversal, implying magnetostatic interactions caused by the presence of soft magnetic α-Fe phase. This result further justified the presence of effective exchange-coupling interaction in the nanocomposite magnet, similar to what had been reported in melt-spun ribbons of nanocomposite where α-Fe phase caused negative δM.[16]

3. Conclusions

In summary, we have reported a bottom-up strategy to synthesize exchange-coupled nanocomposite powder of $Nd_2Fe_{14}B/\alpha\text{-}Fe$ by wet chemical method. The as-synthesized $Nd_2Fe_{14}B/\alpha\text{-}Fe$ exhibits strong exchange-coupled effect as well as enhanced magnetic properties, showing a large coercivity H_c of 12000Gs, remanence M_r of 45 emu/g and an enhanced remanence with M_r/M_{3T}=0.63. We expected that this work not only provides a new route to the synthesis of nanostructured rare-earth magnet, but also able to tune the exchange-coupling effect between the soft and hard magnetic phase.

4. Experimental Section

Neodymium(III) 2,4-pentanedionate $Nd(acac)_3$ (99.9+%), Triethylamineborane $(C_2H_5)_3NBH_3$(95%), 1-Octadecene (ODE, 90%), were purchased from Alfa Aesar. Oleylamine (OAm, > 70%) was purchased from Aldrich. Iron (III) acetylacetonate ($Fe(acac)_3$) was from Beijing Yili Fine Chemical. Iron pentacarbonyl ($Fe(CO)_5$, 98%) was from Xin Ding Peng Fei Chemical Co. in China Anhydrous ethyl alcohol (99.9%), and hexane (99.0%) were purchased from Beijing Chemicals. All syntheses were carried out under air-free conditions, using a standard Schlenk-line setup.

Synthesis of α-Fe NPs: 20 mL ODE and 0.3 ml OAm were degassed at 120 °C for 2 h to remove moisture and impurity. 0.9 ml (6.75 mmol) $Fe(CO)_5$ was quickly injected into the solution and kept for 2 min, then increased to 180 °C at a heating rate of 12 $°Cmin^{-1}$ and kept for 15 min. The α-Fe NPs were precipitated by adding 20 ml ethanol and washed three times with ethanol, then dispersed in hexane.

Synthesis of Nd-Fe-B-oxide/α-Fe precursor: 0.091 g (0.207 mmol) $Nd(acac)_3$ and 0.2g (0.56mmol) $Fe(acac)_3$ was dissolved in 20 ml oleylamine. The solution was degassed at 120 °C for 1 h. α-Fe NPs (13 mg) dispersed in 10 ml hexane were then added into the solution. The solution was kept at 120 °C for 1 h to remove hexane. Then, 13.3 μl (0.08 mmol) $(C_2H_5)_3NBH_3$ was quickly injected. Subsequently, the mixture was heated to 300 °C at a heating rate of 10 $°Cmin^{-1}$ and kept for 1 h before cooling to room temperature. The Nd-Fe-B-oxide/α-Fe precursor with total Nd/Fe ratio tuned by addition of different amount of Nd, Fe precursors and α-Fe as-synthesized was precipitated by ethanol and separated by centrifuging at 10000 rpm for 6 min. The as-prepared composite were dispersed in hexane for further characterization.

Synthesis of $Nd_2Fe_{14}B$/α-Fenanocomposites: A typical procedure for the synthesis of $Nd_2Fe_{14}B$ nanocomposites is as follows: the as-prepared composite were first reduced with stainless steel crucible under Ar + 5% H_2 at 800 °C for 1 h at a heating rate of 20 $°Cmin^{-1}$. Then, 500 mg of Ca powder was ground together with 170 mg of above powder and Nd_2O_3 nano-powder for compensation of neodymium evaporation in glove box. The mixture was wrapped and quickly transferred to a quartz tube that had been flushed with Ar. After that, a reduction & diffusion reaction was carried out at 850 °C for 1.5 h in argon atmosphere and the powder was furnace cooled to room temperature. To remove the CaO and unreacted Ca, the sample was washed twice with 5% acetic acid solution, and then with cold distilled water to remove any traces of acetic acid. Finally, the sample was rinsed with ethanol and dried in vacuum.

Nanocomposites Characterization: The samples were studied by transmission electron microscopy (TEM, TECNAI T20, 300 kV), high-resolution transmission electron microscope (HRTEM, FEI TECNAI F30, 300 kV), field-emission scanning electronic microscopy (SEM, JEOL JSM-7600F, 10 kV), X-ray powder diffraction (XRD, Rigaku D/MAX-2000, Cu Kα) and X-ray Photoelectron Spectroscopy (XPS, Kratos Axis Ultra). Magnetic studies were performed using a Quantum Design SQUID instrument with a field upto 30 kGs. The compositions of the samples were characterized by inductively coupled plasma spectroscopy (ICP) and energy-dispersive X-ray spectroscopy (EDS).

Supporting Information

The size distribution histograms of α-Fe NPs, TEM image for the decomposed products with lower Nd/Fe ratio, and SEM images and XRD patterns for nanocomposites.

Acknowledgements

This work was supported by the National Basic Research Program of China (2010CB934601), NSFC (51125001, 51172005, 90922033, 20806093), the Natural Science Foundation of Beijing (2122022), the Doctoral Program (20120001110078), Natural Science Foundation of Shandong Province (No.ZR2011EMQ001), Technology Project of Qingdao 11-2-4-4-(10)-jch.

Received: ((will be filled in by the editorial staff))
Revised: ((will be filled in by the editorial staff))
Published online: ((will be filled in by the editorial staff))

[1] a) Coehoorn, R.; Demooij, D. B.; Dewaard, C., *J Magn Magn Mater* **1989,** *80*, 101. ; b) Skomski, R.; Coey, J. M. D., *Phys Rev B* **1993,** *48*, 15812.
[2] Zeng, H.; Li, J.; Liu, J. P.; Wang, Z. L.; Sun, S. H., *Nature* **2002,** *420*, 395.
[3] a) Feng, W. C.; Gao, R. W.; Yan, S. S.; Li, W.; Zhu, M. G., *J Appl Phys* **2005,** *98*, 044305. ; b) Yamasaki, M.; Hamano, M.; Mizuguchi, H.; Kobayashi, T.; Hono, K.; Yamamoto, H.; Inoue, A., *Scripta Mater* **2001,** *44*, 1375.
[4] Cui, W. B.; Takahashi, Y. K.; Hono, K., *Adv Mater* **2012,** *24*, 6530.
[5] Liu, W.; Li, X. Z.; Sui, Y. C.; Zhou, J.; Ren, W. J.; Zhang, Z. D.; Sellmyer, D. J., *J Appl Phys* **2008,** *103*.
[6] a) You, C. Y.; Sun, X. K.; Liu, W.; Cui, B. Z.; Zhao, X. G.; Geng, D. Y.; Zhang, Z. D., *Journal of Physics D: Applied Physics* **2002,** *35*, 943. ; b) Niu, P.; Yue, M.; Li, Y.; Huang, W.; Zhang, J., *physica status solidi (a)* **2007,** *204*, 4009.

[7] a) Hyeon, T., *Chem Commun* **2003,** *8*, 927. ; b) Kwon, S. G.; Hyeon, T., *Accounts Chem Res* **2008,** *41*, 1696. ; c) Murray, C. B.; Sun, S. H.; Gaschler, W.; Doyle, H.; Betley, T. A.; Kagan, C. R., *Ibm J Res Dev* **2001,** *45*, 47.
[8] Hong, J. H.; Kim, W. S.; Lee, J. I.; Hur, N. H., *Solid State Commun* **2007,** *141*, 541.
[9] a) Hou, Y.; Sun, S.; Rong, C.; Liu, J. P., *Appl Phys Lett* **2007,** *91*. ; b) Hou, Y. L.; Xu, Z. C.; Peng, S.; Rong, C. B.; Liu, J. P.; Sun, S. H., *Adv Mater* **2007,** *19*, 3349.
[10] Deheri, P. K.; Swaminathan, V.; Bhame, S. D.; Liu, Z.; Ramanujan, R. V., *Chem Mater* **2010,** *22*, 6509.
[11] Farrell, D.; Majetich, S. A.; Wilcoxon, J. P., *The Journal of Physical Chemistry B* **2003,** *107*, 11022.
[12] Peng, S.; Wang, C.; Xie, J.; Sun, S. H., *J Am Chem Soc* **2006,** *128*, 10676.
[13] a) Kneller, E. F.; Hawig, R., *Ieee T Magn* **1991,** *27*, 3588. ; b) Kneller, E. F.; Hawig, R., *Ieee T Magn* **1991,** *27*, 3. ; c) Skomski, R.; Coey, J. M. D., *Phys Rev B* **1993,** *48*, 15812. ; d) Schrefl, T.; Kronmüller, H.; Fidler, J., *J Magn Magn Mater* **1993,** *127*, L273.
[14] Kelly, P. E.; O'Grady, K.; Mayo, P. I.; Chantrell, R. W., *Ieee T Magn* **1989,** *25*, 3881.
[15] a) Zeng, H.; Sun, S. H.; Vedantam, T. S.; Liu, J. P.; Dai, Z. R.; Wang, Z. L., *Appl Phys Lett* **2002,** *80*, 2583. ; b) Rong, C. B.; Zhang, H. W.; Shen, B. G.; Liu, J. P., *Appl Phys Lett* **2006,** *88*, 42504.
[16] Wang, Z.; Zhou, S.; Zhang, M.; Qiao, Y.; Wang, R., *J Appl Phys* **1999,** *86*, 7010.

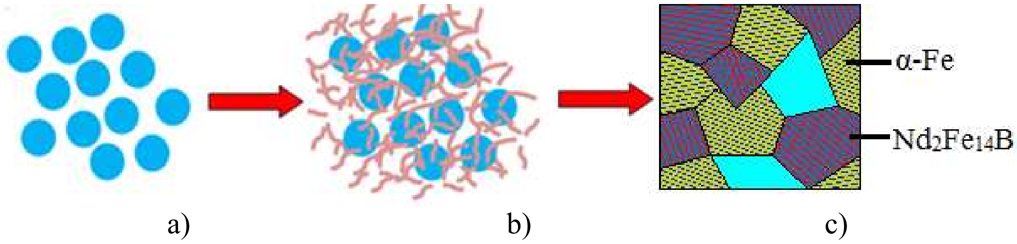

Scheme 1. Schematic illustration of $Nd_2Fe_{14}B$/α-Fe nanocomposites synthesized by wet chemical method. (a) monodispersed α-Fe NPs; (b) composites of α-Fe evenly embedded in net-like Nd-Fe-B-oxide matrix; (c) $Nd_2Fe_{14}B$/α-Fe nanocomposites obtained by thermal reductive diffusion process.

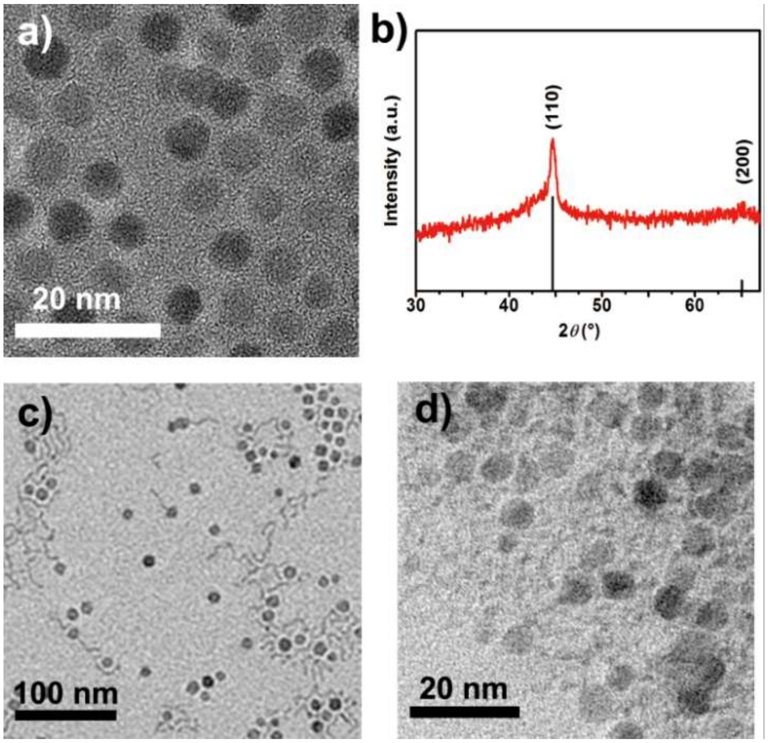

Figure 1. (a) TEM image, (b) XRD pattern of 5 nm monodisperse α-Fe NPs, (c, d) TEM images of Nd-Fe-B-oxide/α-Fe precursor with total Nd/Fe ratio of 2.6/10.

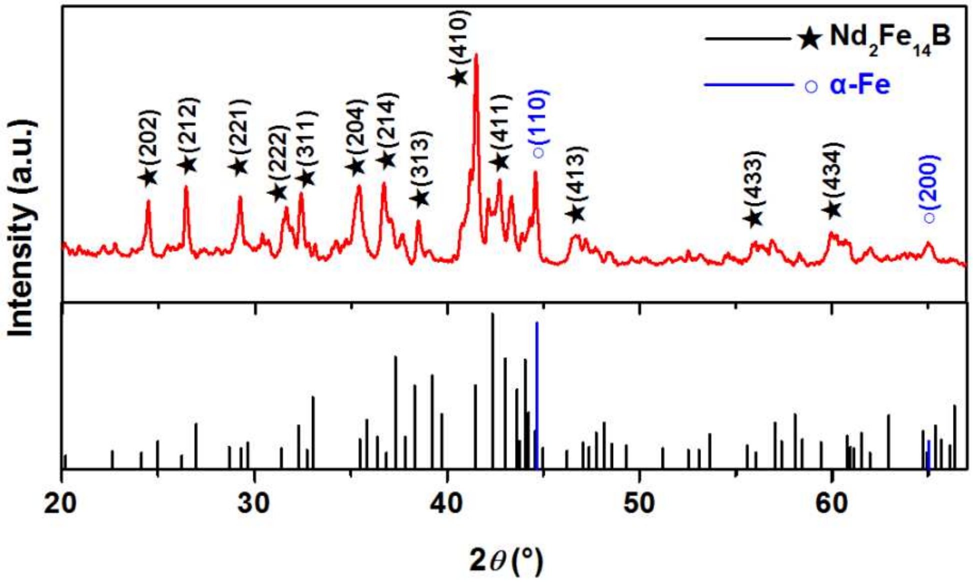

Figure 2. XRD patterns of the precursor after reduction and diffusion process at 850 °C for 1.5 h. (JCPDS 36-1296) and α-Fe phase (JCPDS 06-0696).

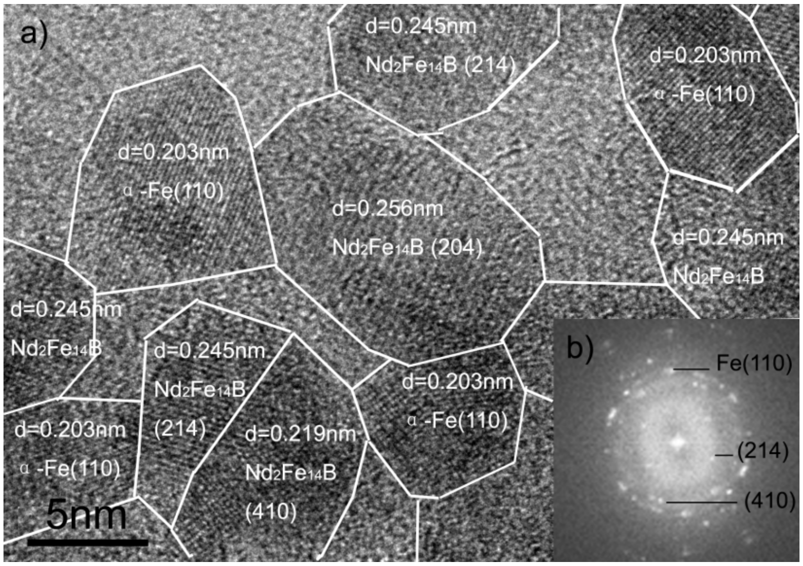

Figure 3. (a) HRTEM image of $Nd_2Fe_{14}B$/α-Fe nanocomposite prepared by reductive annealing of Nd-Fe-B-oxide/α-Fe precursor. The lattice spacing of 0.203 nm corresponds to the (110) planes of α-Fe, and the lattice spacing of 0.219nm, 0.245nm and 0.256 nm assigns to the (410), (214) and (204) planes of $Nd_2Fe_{14}B$, respectively. (b) The corresponding fast Fourier-transform (FFT) pattern of $Nd_2Fe_{14}B$/α-Fe nanocomposite (inset).

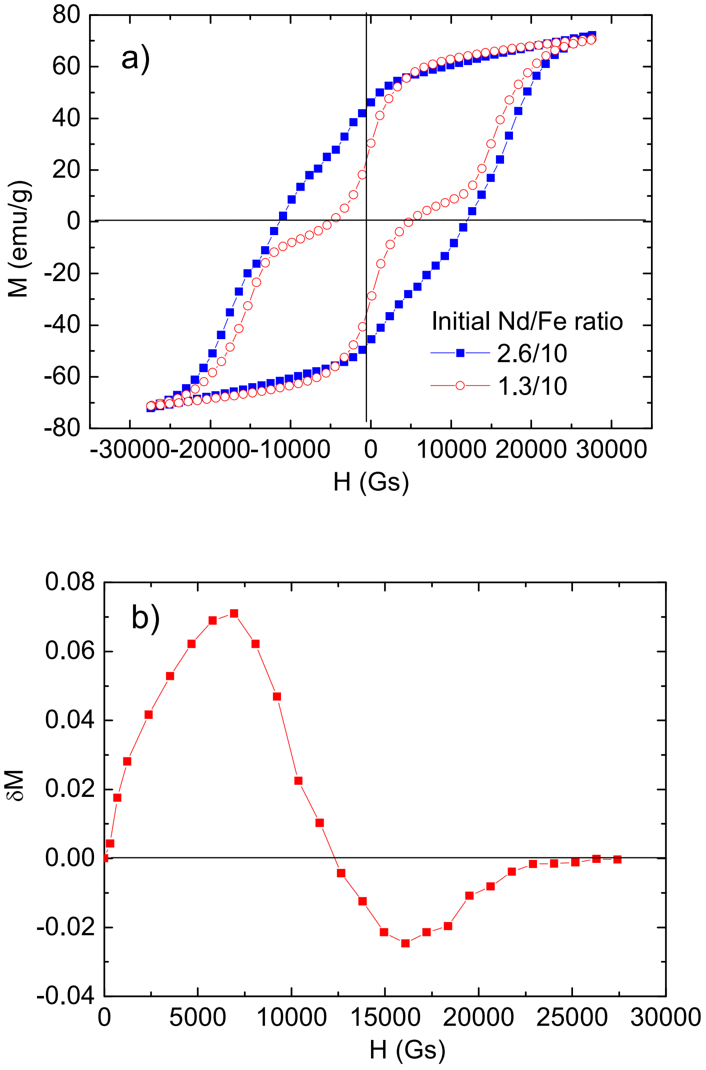

Figure 4. (a) Hysteresis loops at room temperature for $Nd_2Fe_{14}B/\alpha$-Fe nanocomposite prepared from Nd-Fe-B-oxide/α-Fe precursor with total Nd/Fe ratio of (square) 2.6/10 and (circle) 1.3/10. The blue square loop shows single–phase-like behavior, indicting effective exchange-coupled behavior while the red circle hysteresis showed two-phase behavior. The kink at low field is related to the soft phase α-Fe magnetic reversal; (b) δM-H plot of nanocomposites at Nd/Fe ratio of 2.6/10.

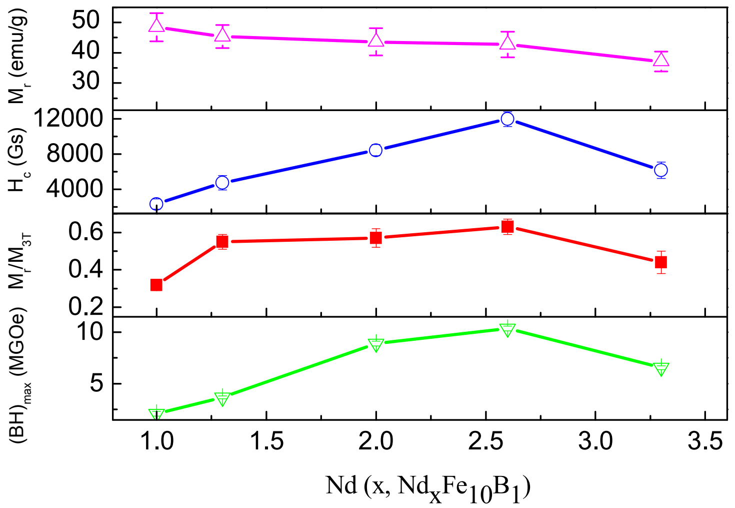

Figure 5. Change of coercivity, remanence and M_r/M_{3T} in the $Nd_2Fe_{14}B$/α-Fe nanocomposites prepared from Nd-Fe-B-oxide/α-Fe precursor with total Nd/Fe ratio of $Nd_xFe_{10}B_1$. The error bar represents the standard deviation obtained from 3 samples.

TOC

Exchange-coupled nanocomposites of $Nd_2Fe_{14}B/\alpha$-Fe are successfully synthesized by thermal decomposition and reductive annealing process. An Nd-Fe-B-oxide/α-Fe precursor of α-Fe NPs embedded in net-like Nd-Fe-B-oxide matrix is formed. The phase size, composition as well as magnetic properties can be readily tuned by changing the ratio between Nd-Fe-B-oxide and α-Fe. The optimum properties shows coercivity of 12000Gs and an enhanced remanence of M_r/M_{3T}=0.63.

Keyword Exchange-coupled, nanocomposites, NdFeB, reductive annealing process, chemical synthesis

Lianqing Yu, Ce Yang, Yanglong Hou*

Exchange-coupledNd$_2$Fe$_{14}$B/α-Fe Nanocomposites: Chemical Synthesis and Magnetic Properties